ORIGINAL PAPER

Comparative analysis of cigarette smoke induced cellular proteome distributions on bovine aortic endothelial cells

Jiho Min[1,*], Ji-Young Ahn[2,*], Simranjeet Singh Sekhon[2], Yoon Mi Jin[3], Hyun-Ju Um[2], Inho Jo[3] & Yang-Hoon Kim[2]

Abstract Cigarette smoke is a contributory factor for the cardiovascular disease, lung diseases and cancers as the dominant illnesses. The proteomic analysis of bovine aortic endothelial cells (BAECs) exposed to cigarette smoke has been performed in the broad (Non-linear pH 3-11) and narrow (Linear pH 4-7) range by using two-dimensional gel electrophoresis (2-DE). Out of an average 950 spots observed in 2-DE gels under pH 3-11, the expression level of 25 proteins significantly increased with an increase of cigarette smoke extract (CSE) level, whereas 21 proteins were strongly down-regulated. In narrow (4-7) pH range analysis, 80 proteins showed a significant change in expression level as compared with control. Some of the proteins were found to show similar spot intensity patterns in both the linear (4-7) and non-linear (3-11) pH ranges. Most of the proteins identified in both pH conditions were found to be involved in apoptosis, inflammation, transcription modulator, signal transduction pathway, ROS production, cell proliferation and extracellular structure formation. In addition, extracellular structural proteins also responded to apoptotic signaling as an indicator. The findings of the present study can be used as an early biomarker to indicate the risks of cigarette smoke related diseases and also in the design of new therapeutic and diagnostic approaches to control these diseases.

Cigarette smoking is a serious health problem known to be associated with oxidative stress[1], activation of the inflammatory systems and vascular abnormalities[2]. The majority of individuals chronically exposed to cigarette smoke eventually result in cardiovascular disease, lung diseases and cancers as the dominant illnesses[3,4]. During the last few years, many research efforts have focused extensively on the role of cigarette smoking as a cause of cardiovascular disease in the epidemiologic and biomedical mechanisms[5-10]. However, despite the major cardiovascular health implications of cigarette smoke exposure, their role in cardiovascular cell dysfunction that leads to cardiovascular disease development is still being explored. The cigarette smoke generates more than 4000 chemical compounds which can lead to alterations such as post-transcriptional modifications and protein cellular functions. Therefore, it is important to explore the protein responses to cigarette smoke in addition to changes at the mRNA levels[11]. Moreover, identification of the cigarette smoke-induced/reduced proteins would provide useful information in understanding the role of endothelial cells in cardiovascular homeostasis under normal conditions and in disease states.

Previous studies[12,13] probing smoking-effects have focused on few selected proteins, and traditional protein identification techniques such as Western blott-

[1]Graduate School of Semiconductor and Chemical Engineering, Chonbuk National University 664-14, 1-Ga, Duckjin-Dong, Duckjin-Gu, Jeonju 561-156, Korea
[2]Department of Microbiology, Chungbuk National University 52 Naesudong-Ro, Heungduk-Gu, Cheongju 361-763, Korea
[3]Department of Molecular Medicine and Ewha Medical Research Institute, Ewha Womans University Medical School, 911-1 Mok-6-Dong, Yangchun-gu, Seoul 158-710, Korea
*These authors contributed equally to this work.
Correspondence and requests for materials should be addressed to Y.-H. Kim (✉ kyh@chungbuk.ac.kr) & I. Jo (✉ inhojo@ewha.ac.kr)

Springer

ing. These have resulted in identification of only a few numbers of responsive proteins in endothelial cells[14]. Also, these techniques can identify only one protein at a time, and are limited by the availability and quality of specific antibodies. Recently, there have been some reports on the comprehensive view of the physiological state and individual's susceptibility to the adverse effect of cigarette smoke using proteomic tools[15,16]. However these approaches relating quantitative dynamic analysis and the molecular/cellular mechanisms are still at an early stage of development. Nevertheless, the extended proteomics (along with protein sequence data and enhanced MS technology) have been proposed as a powerful tool for the predictions and delineation of various regulatory mechanisms. A new approach has been focused on the toxicological changes relevant to cellular phenomenon such as cell proliferation, chronic inflammation, and induction/inhibition of apoptosis. Toxicoproteomic approach is currently being employed to evaluate the protein changes associated with these functional changes[17,18].

In the present study, the overall protein expression pattern of bovine aortic endothelial cell (BAEC) was studied during the treatment of cigarette smoke extract (CSE). Since the cigarette smoking is now understood as a major risk factor for endothelial dysfunction[19], the detailed proteome analysis results could be useful in understanding the disease pathway and the function of molecular disease markers. Moreover, bovine endothelial cells are an economical alternative suitable for the studies of endothelial function and endothelial metabolism, especially in co-culture of species-matched bovine arterial smooth muscle cells[20].

Comparative research of its proteomic responses against the different concentration levels of cigarette smoke extract was performed by 2D-gel and image analysis. A significantly different protein expression pattern between the control and the CSE-exposed BAEC was observed and demonstrated in detail on the synthesis level. Proteins and peptide masses were analyzed by automated matrix-assisted laser desorption/ionization time-of-flight (MALDI-TOF) mass spectrometry and were matched with the theoretical peptide masses in the ExPASy database, and their functional characteristics in the cellular metabolisms were then elucidated. To understand CSE-induced changes in the BAECs proteome, we focused on the identification of disappearing and appearing spots, as well as up- and down-regulation of spot intensities in broad nonlinear (3-11) and narrow linear (4-7) pH range conditions.

Effect of CSE and protein expressions on an immobilized pH 3-11 non-linear wide range gradient strip

Due to the CSE-induced differences in protein expression related oxidative stress and apoptosis dose-dependence[21], BAECs was treated with 3 and 5% CSE for 24 h. For each protein sample, 2-D SDS-PAGE analysis was repeated 4-8 times, and after silver-staining an average 2-DE gel image was constructed for comparative analysis using the ImageMaster software (Amersham Pharmacia Biotech, NJ, USA). Concentration dependent whole protein profile was compared with untreated BAECs. Initially, 2-DE was carried out on total whole-proteins using a broad range pH (3-10) immobilized pH gradient for the first dimension. Figure 1 shows a typical 2-DE profile in the pH range from 3 to 11. Approximately, 950 spots were visualized on each averaged gel image; in control (0%), 3% and 5% CSE- treated BAECs (Figure 1). The spot
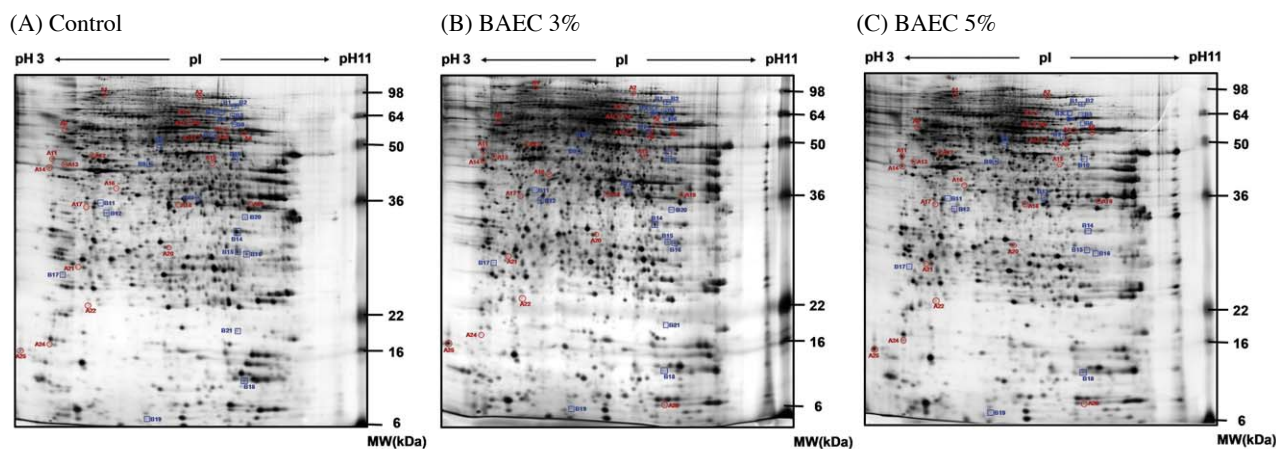

Figure 1. Silver stained 2-D SDS-PAGE gels showing 46 protein spots listed in Table 1. The red circle indicated induced proteins [○]; and the blue indicated repressed proteins [□]. Control, (A); CSE 3% treatment (B); CSE 5% treatment (C).

intensity was calculated for each spot, and spot with fold changes in spot intensity compared with the control value 1 for the CSE-untreated BAEC. A total of 46 unique proteins were identified and are listed in Table 1. Eventually, the expression ratios above 1 indicate induction, and those below 1 indicate repression. The results were mainly focused on the following proteomic behavior of CSE: (i) the synthetic levels of 25 proteins (A1-A25) were significantly induced after exposure to 3% CSE and the high levels were maintained in proportion to an increase of CSE level to 5% and (ii) 21 proteins (B1-B21) were significantly repressed for a prolonged exposure period at both concentrations (3% and 5%) of CSE. Moreover, proteins which were proportionally up-regulated by more than 10-fold or repressed by less than 0.1-fold in the difference between control and CSE-treated BAECs were highlighted.

Effect of CSE and protein expressions on an immobilized pH 4-7 linear narrow range gradient strip

To understand the effect of CSE on BARCs proteome in detail we also performed an analysis in the narrow acidic (4-7) pH. According to a previous proteome study, not only wide pH gradient such as 3-11, which can give an overview of the total protein expressions of cells are in demand but overlapping narrow immobilized pH gradients are also to be used for more specialized and detailed research and in micropreparative separations[22]. In this pH range, a total of 80 proteins showed a significant change in the expression level when compared with control. Spots with fold changes in spot intensity by more than 1 as well as by less than 1 were analyzed first and are tabulated in Table 2. Out of them, 43 proteins (a1-a43) were up-regulated and 12 proteins (b1-b12) were down-regulated upon treatment with CSE. More interestingly, some proteins showed very similar spot intensity change patterns in the two pH ranges, linear gradient 4-7 and non-linear gradient 3-11, (Interferon-alpha/beta receptor chain (IFNAR), Vascuolar ATP synthase subunit H (ATP6V1H), Glial fibrillary acidic protein (GFAP), Cartilage oligomeric matrix protein (COMP) and Adenosine deaminase (ADA), see Table 1 and 2).

Then, 25 differentially appearing and disappearing protein spots were identified and are listed in Table 3. Moreover, Figure 2 displays the 2D pattern of BAECs treated with 3% and 5% CSE and analyzed in the narrow (4-7) pH range. A number of protein features were either lost or appeared upon the change in concentration of CSE. 6 proteins (F1-F6) present on basal gels were not detectable following treatment with CSE, and 17 proteins could not be identified on control gels but were found on CSE treated gels (C1-C11 and D1-D6). The other 2 protein features (E1 and E2) were present on basal, but were down-regulated on 3% CSE gels but disappeared under 5% CSE condition.

Some examples of change in spot features are shown in Figure 3. Figure 3A and B illustrates 2 set of protein features that appear and disappear upon CSE treatment. In Figure 3A, proteins identified as secreted protein acidic and rich in cysteine (SPARC, C9), 40S ribosomal protein SA (RPSA, C10), Calbidin (CALB1, C11) and similar to epsilon isoform of 14-3-3 protein (D1), appears to be expressed or activated by CSE treatment. Figure 3B shows that protein features, marked as F1, F2, F3, and F6 that disappear upon CSE treatment, correspond to Collectin-43 precursor (CL43), Actin, aortic smooth muscle (ACTA2), Myocilin (MYOC), and A-kinase anchor protein 5 (AKAP5), respectively.

Discussion

Comparative proteomic analyses of cigarette smoke-responsive proteins between 3% and 5% CSE exposure were performed by using linear and nonlinear 2-DE analysis, and significant expression differences were found. To improve the resolution and enhance the detection of low abundance proteins, we used two difference pH gradient conditions (pH 3-11 non-linear wide range and pH 4-7 linear narrow range gradient strip). Eventually, out of an average 950 spots observed in 2-DE gels under pH 3-11, the expression level of 25 proteins significantly increased with an increase of cigarette smoke extract (CSE) level, whereas 21 proteins were strongly down-regulated.

Protein-overexpression involved in apoptosis

To obtain a more accurate understanding of some proteins due to exposure to CSE, we first focused on Rho-GTPase-activating protein (spot A15). This protein has been significantly enhanced when exposed to low concentration of CSE (3%) and the high level of expression has been maintained at exposure to 5% CSE. The Rho family of small GTPase is involved in several important cellular processes, for example, gene-expression regulation, molecular travelling between subcellular organelles, cell proliferation and apoptosis[23]. The overexpression of Rho-GTPase has earlier been reported to contribute to the tumorization[24]. Moreover, it can be regulated both positively and negatively; through guanine nucleotide exchange factors (GEFs) and the Rho-GTPase activating proteins (RhoGAPs). Being the negative regulator, Rho-GTPase activating proteins (RhoGAPs) can deprecate the function of Rho

Table 1. Identification of CSE related proteins in a broad pH range 3-11 (NL, non-linear).

Spot No.	Gene name	Protein name	pI	MW (kDa)	Accession number[a]	Sequence coverage[b] (%)	Protein level ratio (fold change)[c]		
							Control/ Control	CSE 3%/ Control	CSE 5%/ Control
A1	ALS2CR8	Amyotrophic lateral sclerosis 2 chromosomal region candidate gene 8 protein homolog	5.4	78.136	Q58CW6	72.3	1	1.13	5.66
A2	ITGB2	Integrin beta-2 (CD18 antigen)	6.05	84.400	P32592	74.2	1	3.71	5.59
A3	LOC533212	Similar to obscurin, cytoskeletal calmodulin and titin-interacting RhoGEF	6.3	68.125	76645255	71.2	1	4	6.42
A4	PMPCB	Mitochondrial processing peptidase beta subunit, mitochondrial precursor (Beta-MPP)	6	54.28	Q3SZ71	69.8	1	2.08	8.56
A5	LOC505426	similar to spermatogenesis associated 13 isoform 1	6.3	64.207	76631577	72.6	1	1.56	6.23
A6	IFNAR1/IFNAR	Interferon-alpha/beta receptor alpha chain (IFN-alpha-REC)	5.1	63.819	Q04790	68.8	1	1.53	6.87
A7	ATP6V1H	Vacuolar ATP synthase subunit H	6.18	55.852	O46563	65.4	1	3.09	9.82
A8	MGC128737	Similar to WD repeat domain 5B	6.81	52.467	Q3MHJ1	71.2	1	4.06	6.87
A9	ROCK1	Rho-associated protein kinase 1 [Fragment]	5.91	52.386	Q8MIT6	75.6	1	1.93	6.07
A10	TUFT1	Tuftelin 1	5.66	44.343	P27628	70.6	1	3.08	5.58
A11	PSEN2	Presenilin-2 (PS-2)	4.51	50.271	Q9XT96	75.4	1	7.14	8.58
A12	GFAP	Glial fibrillary acidic protein, astrocyte (GFAP)	5.36	49.512	Q28115	74.6	1	2.12	7.03
A13	COMP	Cartilage oligomeric matrix protein [Fragment]	4.2	48.962	P35445	68.5	1	2.49	**10.69**
A14	CALU	Calumenin [Precursor]	4.41	37.083	Q3T0K1	66.5	1	6.27	6.91
A15	LOC508266	Rho-GTPase-activating protein 2	6.5	53.109	76609541	74.3	1	15.4	**15.45**
A16	MAPKAPK3	MAP kinase-activated protein kinase 3	7.58	43.316	Q3SYZ2	63.5	1	2.25	8.33
A17	ADA	Adenosine deaminase (Adenosine aminohydrolase)	5.3	40.789	P56658	61.2	1	3.05	**15.04**
A18	DNMT2	DNA methyltransferase 2 isoform	6.2	42.999	61554791	74.2	1	7.95	**29.74**
A19	LOC513855	Alcohol dehydrogenase [NADP+]	7.6	35.791	76674321	72.8	1	9.23	**10**
A20	LOC614696	similar to Ellis-van Creveld syndrome protein (DWF-1)	5.5	33.161	76683470	77.2	1	1.82	5.18
A21	M6PR	Cation-dependent mannose-6-phosphate receptor [Precursor]	5.44	31.201	P11456	65.3	1	6.26	8.19
A22	GCSH	Glycine cleavage system H protein, mitochondrial [Precursor]	5.13	18.791	P20821	68.9	1	1.45	**10.49**
A23	GUCA1A	Guanylate cyclase-activating protein 1	4.40	23.510	P46065	71.1	1	3.36	6.73
A24	CABP5	Calcium-binding protein 5	4.34	19.628	Q9N1Q8	72.1	1	2.9	5.33
A25	RPS27A	Ubiquitin	6.56	8.565	P62990	69.9	–	1	1.85
B1	C22orf19, KIAA0983	Uncharacterized protein C22orf19, NF2/meningioma region protein pK1.3, Placental protein 39.2	6.41	78.536	Q13769	68.8	1	0.88	0.2
B2	LOC617928	similar to butyrophilin, subfamily 2, member A1 isoform 1 precursor	7.00	77.253	76651055	72.4	1	0.58	0.24
B3	PPCK1	Phosphoenolpyruvate carboxykinase, cytosolic [GTP]	6.30	69.35	Q8HYZ4	67.7	1	0.56	0.17
B4	LOC511188	similar to eyes absent 1 isoform c isoform 1	6.8	77.754	76660014	66.5	1	0.44	0.21
B5	NR4A1	Orphan nuclear receptor NR4A1	6.82	64.437	Q0V8F0	71.1	1	0.6	0.22
B6	SARS2	Seryl-tRNA synthetase, mitochondrial [Precursor]	7.25	58.296	Q9N0F3	72.5	1	0.25	**0.025**
B7	DNPEP	Aspartyl aminopeptidase	6.45	51.828	Q2HJH1	73.8	1	0.8	0.23
B8	LAP3	Cytosol aminopeptidase	6.07	56.289	P00727	79.8	1	0.48	0.15
B9	GNAI1	Adenylate cyclase-inhibiting G alpha protein	5.69	40.361	P63097	69.9	1	0.64	0.23
B10	LOC505945	similar to serine/arginine-rich protein specific kinase 2	7.2	48.336	76615230	64.2	1	0.47	0.17
B11	LOC510572	similar to cell division cycle 37 homolog (S. cerevisiae)-like 1 isoform 2	5.3	38.85	76624280 (Q5IVJ2)	68.5	1	0.67	0.18
B12	ACTB	Actin, cytoplasmic 1	5.29	41.737	P60712	71.3	1	0.24	0.21

Table 1. Continued.

Spot No.	Gene name	Protein name	pI	MW (kDa)	Accession number[a]	Sequence coverage[b] (%)	Protein level ratio (fold change)[c]		
							Control/Control	CSE 3%/Control	CSE 5%/Control
B13	SAG	S-arrestin	6.10	45.28	P08168	70.8	1	0.92	**0.068**
B14	NDUFS3	NADH dehydrogenase [ubiquinone] iron-sulfur protein 3, mitochondrial [Precursor]	6.55	30.284	P23709	75.3	1	0.1	**0.05**
B15	UPK3B	Uroplakin-3B [Precursor]	6.95	30.587	Q864V4	76.5	1	0.37	0.17
B16	TMED9	Transmembrane emp24 domain-containing protein 9 [Precursor]	7.76	27.298	Q3T133	64.2	1	0.73	**0.05**
B17	RPSA	40S ribosomal protein SA	4.80	32.77	P26452	62.2	1	0.24	0.24
B18	MFAP5	Microfibrillar-associated protein 5 [Precursor]	6.81	19.080	Q28022	68.5	1	0.45	0.15
B19	LOC504565	Similar to STIP1 homology and U-box containing protein 1	5.2	8.135	76652356	66.5	1	0.52	0.17
B20	BCL2L14	Annexin A2	6.90	38.481	P04272	71.2	1	1	ND
B21	DHFR	Dihydrofolate reductase	6.20	21.604	P00376	74.4	1	**0.07**	ND

[a]Accession code refers to the SWISS-2DPAGE database; [b]Mass tolerance in protein identification through PMF experiment was 10 ppm; [c]Protein expression level in each growth phases compared with N4 phase. Expression level in N4 phase was set at 1; ND: Non-Detected.

proteins by improving the GTPase activity, which modulates the proapoptotic cellular processes, consisting of signal-caspases for programmed cell death[25,26]. In the present work, the abundance of a spot containing Rho-GTPase-activating protein has been observed to drastically induce by 15-fold when cells were exposed to 3% CSE thereby identifying it as a potential marker in apoptotic cellular response.

Many metabolic agents that induce apoptosis are either oxidants or stimulators of cellular oxidative metabolism. It is currently believed that reactive oxygen species (ROS) and the resulting oxidative stress play a pivotal role in apoptosis[21]. In line with previous studies, oxidative stress seems to be closely linked to the accumulation of alcohol dehydrogenase (ADH). ADH is the primary enzyme responsible for the oxidation of ethanol that occurs in many organisms and facilitates the inter-conversion between alcohols and aldehydes or ketones with the reduction of nicotinamide adenine dinucleotide (NAD+ to NADH). The spot of A19 was barely detectable in control (Figure 1A), but a significant spot appeared after exposure to 3 and 5% CSE. Taken together, RhoGAPs, and the resulting ADH induction can be a part of a signal transduction pathway leading to apoptotic cell death.

Protein-overexpression involved in inflammation

The differently expressed proteins listed here can be classified into two groups. The first group which includes RhoGAPs and ADH has already been considered as an apoptotic factor. Both of them responded drastically when cells were exposed to lower concentration (3%) of CSE and maintained their expression activity in 5% CSE exposure. Interestingly, others including Adenosine deaminase (ADA, A17), DNA methyl transferase (DNMT2, A18) and Glycine cleavage system H protein (GCSH, A22), were accelerated to express over 10-fold following 5% CSE treatment. So it is assumed that the second group may be involved in some different biological category, which responds to high level of CSE expose, in terms of secondary apoptosis and inflammatory. It has been reported[27] that the excessive presence of signal of apoptotic and the accumulation of dying cells can lead to the cellular inflammation responses. That is, because the failed clearance of apoptotic cells was believed to contribute to the pathological processes such as inflammation and they tried to understand how apoptotic cells are processed and cleared and how this process affects the recruit inflammation process through caspase activity anslysis. However, we show that Adenosine deaminase, DNA methyltransferase and Glycine cleavage system H protein were expressed in high abundance at 5% CSE condition, and they may be involved

Table 2. List of differentially expressed proteins in a narrow pH range 4-7 (L, linear).

Spot No.	Gene name	Protein name	pI	MW (kDa)	Accession number[a]	Sequence coverage[b] (%)	Control/Control	CSE 3%/Control	CSE 5%/Control
1	HSP90B1	Endoplasmin precursor	4.8	92.427	27807263	85.43	1	2.25	3.07
a2	DPP6	Dipeptidyl aminopeptidase-like protein 6	6.0	96.558	27806657	75.46	1	3.14	3.23
a3	CAST	Calpain inhibitor	4.9	75.844	1352417	91.24	1	1.80	2.41
a4	UMOD	Uromodulin precursor	4.8	69.899	27806359	81.23	1	1.52	2.94
a5	NEFL	Neurofilament light polypeptide	4.6	62.646	27806523	77.35	1	1.38	1.67
a6	IFNAR1	Interferon alpha/beta receptor 1	5.1	63.819	27807001	84.51	1	1.61	3.40
a7	bcnt	Endonuclease	5.3	66.266	22779307	72.13	1	2.12	3.81
a8	Ang-1	Angiopoietin-1	6.3	55.557	3668414	76.38	1	1.41	2.87
a9	ALCAM	CD166 antigen precursor	6.4	64.766	NP_776663	85.24	1	2.21	3.05
a10	ATP6V1H	Vacuolar-type proton ATPase subunit H	6.3	55.933	O46563	81.67	1	3.14	4.55
a11	COMP	Cartilage oligomeric matrix protein	4.2	48.962	262073096	92.06	1	2.64	4.17
a12	CLIC5	Chloride intracellular channel protein 5	4.5	48.959	27805879	82.64	1	3.19	5.43
a13	VIM	Vimentin	5.2	53.677	P48616	72.19	1	2.32	4.30
a14	LAP3	Cytosol aminopeptidase	5.7	53.002	1703281	85.11	1	1.91	5.21
a15	CK-19	Cytokeratin 19	4.9	43.885	1197196	91.31	1	2.45	3.77
a16	DES	Desmin	5.2	52.562	BAA25133	72.36	1	1.33	1.61
a17	GFAP	Glial fibrillary acidic protein	5.3	49.453	28849921	77.81	1	2.17	2.41
a18	SERPINB6	Serpin B6	5.4	42.561	27807517	76.25	1	2.04	2.35
a19	ADA	Adenosine deaminase	5.3	40.920	27806933	81.24	1	2.78	4.61
a20	PPM1B	Protein phosphatase 1B	5.1	42.834	27806079	82.25	1	1.50	2.02
a21	TPM1	Tropomyosin alpha-1 chain	4.7	32.695	61888866	82.49	1	2.66	3.89
a22	c-fos	c-Fos	4.8	40.738	32481980	74.35	1	2.21	4.12
a23	MUC15	Mucin-15 precursor	4.9	35.716	41386723	92.24	1	3.00	3.21
a24	BC1	Bovine cytochrome Bc1 complex with stigmatellin and antimycin	6.5	27.288	51247185	89.35	1	1.96	2.82
a25	M6PR	Cation-dependent mannose-6-phosphate receptor precursor	5.4	31.202	28461185	93.21	1	2.82	3.91
a26	ANPEP	Aminopeptidase	4.8	27.281	31076600	82.37	1	2.54	3.23
a27	CAPNS1	Calpain small subunit 1	5.1	27.932	27806277	84.51	1	1.32	1.61
a28	KCNRG	Putative potassium channel regulatory protein	7.0	30.370	45430039	79.15	1	2.31	5.52
a29	BoLA-DRB3	MHC class II antigen	6.3	30.589	21672261	77.65	1	1.71	2.52
a30	CYP2C8	Cytochrome P450 2C	5.5	26.549	30523218	75.91	1	1.61	2.72
a31	apoA-1	Apolipoprotein A-I	5.6	28.432	245563	78.61	1	4.52	10.80
a32	CRYBA4	Beta-crystallin A4	5.8	23.861	27806951	81.05	1	3.69	8.72
a33	PCTP	Phosphatidylcholine transfer protein	6.2	24.643	27807327	88.27	1	2.31	6.78
a34	GUCA1A	Guanylyl cyclase-activating protein 1	4.4	23.511	27806991	83.61	1	1.82	5.31
a35	PDCL	Phosducin-like	4.8	25.058	27807471	81.34	1	2.33	5.15
a36	Vsnl1	Visinin-like 1	5.0	22.143	6981708	82.04	1	1.38	2.17
a37	TCRG1	T cell receptor gamma C1	6.5	23.354	49424746	72.69	1	1.95	3.58
a38		Immunoglobulin variable region	4.7	14.570	2353750	78.36	1	1.46	3.91
a39	esss	Mitochondrial NADH:ubiquinone oxidoreductase ESSS subunit	4.8	15.403	23954189	79.14	1	2.00	3.97
a40	RPLP2	60S acidic ribosomal protein P2	4.5	11.702	27807523	83.51	1	1.86	4.49
a41	stat3	Signal transducer and activator of transcription 3	4.7	12.552	44804303	95.21	1	1.30	2.91
a42	TBCA	Tubulin-specific chaperone A	5.4	12.707	28461233	85.21	1	2.33	2.56

Table 2. Continued.

Spot No.	Gene name	Protein name	pI	MW (kDa)	Accession number[a]	Sequence coverage[b] (%)	Protein level ratio (fold change)[c]		
							Control/ Control	CSE 3%/ Control	CSE 5%/ Control
a43	S100A4	Protein S100-A4	5.9	11.807	NP_777020	72.33	1	1.21	4.15
a44	GNGT1	Guanine nucleotide-binding protein G (T) subunit gamma-T1 precursor	4.8	8.544	27805893	82.66	1	3.61	6.16
b1	BoLA-DQB	MHC class II	6.1	28.417	1018981	76.92	1	0.41	0.23
b2	TXNRD1	Thioredoxin reductase 1, cytoplasmic	6.1	54.724	O62768	85.12	1	0.81	0.75
b3	LOC514910	similar to myosin, heavy polypeptide 6, cardiac muscle, alpha	6.6	43.823	76623898	91.32	1	0.90	1.55
b4		5-lipoxygenase	5.6	50.001	13235074	85.23	1	0.8	0.52
b5	CDK11	PITSLRE protein kinase beta 1	5.5	49.530	56119132	72.15	1	0.42	0.35
b6	BFSP2	Beaded filament structural protein 2, phakinin	5.6	45.950	118403614	73.61	1	0.53	0.48
b7	APOE	Apolipoprotein E	5.5	35.980	Q03247	75.81	1	0.42	0.56
b8	TKDP1	trophoblast Kunitz domain protein 1	6.0	38.255	7341320	79.38	1	0.91	0.32
b9		acidic ribosomal phosphoprotein PO	5.3	32.377	2293577	85.67	1	0.50	0.43
b10	PPA1	Pyrophosphate phospho-hydrolase	5.3	32.844	P37980	88.09	1	0.35	0.26
b11	GAP43	growth-associated protein 43	4.7	25.082	42733594	72.68	1	0.57	0.88
b12	PNP	Calf Spleen Purine Nucleoside Phosphorylase (Pnp)	5.9	32.094	51247896	79.10	1	0.38	0.42

[a]Accession code refers to the SWISS-2DPAGE database; [b]Mass tolerance in protein identification through PMF experiment was 10 ppm; [c]Protein expression level in each growth phases compared with N4 phase. Expression level in N4 phase was set at 1.

in phagocytic clearance process upon the induction of apoptosis and inflammation.

We observed an induction of Adenosine deaminase (ADA) to a level of 15.4-fold versus controls. Adenosine deaminase (ADA) consists of two major principal isoenzymes: ADA1 and ADA2. In particular, ADA2 has a greater connection with adenosine and has been mainly found in macrophages[28]. Macrophages release ADA2 when stimulated by the presence of pathological microorganism and are likely to contribute to the control of inflammation because accelerated ATP metabolism occurs in chronic inflammatory diseases[29]. Eventually, the induction of ADA proteins by CSE-expose in high levels can also induce differentiation of monocytes and stimulates proliferation of T_h-cells and other macrophages that are associated with inflammation pathway.

DNA methyl transferase (DNMT, A18) displayed significant induction in abundance of about 8-fold for 3% CSE and 30-fold for 5% CSE. It has been reported that the inflammatory cytokine IL-6 is able to induce the maturation and differentiation of immune cells and is also capable of inducing DNMT expression and its activity[30]. Moreover, they demonstrated that the biological activity of IL-6 might be also modulated by DNMT in a cooperative manner. However, we postulate that the high-dose exposure to CSE directly affect the inflammatory cells, which can lead to induction of DNMT by releasing IL-6.

Finally, Glycine cleavage system H protein (GCSH, A22) showed more than 10-fold abundance compared to control level while cellular exposure to 5% CSE. The glycine cleavage system, also known as the glycine decarboxylase multienzymatic complex, is composed of four mitochondrial components (the T-, P-, L-, and H- proteins)[31]. As a crucial part of the glycine/serine metabolic processes, this system can be regenerated by the oxidized H-protein activity. The mechanism of the immunosuppressive effect as anti-infflammatory immunonutrient has been reported[32] and in their study, glycine acts on inflammatory cells such as macrophages to suppress activation of transcription factors and inflammatory cytokines. The transcriptional activator of GCSH expression in genetic study is not known well, but GSCH induced on 2-DE in the present study may promote more rapid glycine consumption, thereby triggering apoptosis and inflammation process.

Down regulation of transcription modulator

We observed significant repression of Seryl-tRNA synthetase (SARS, B6) to a level of about 0.25 and 0.025 fold (relative to control) at 3% and 5% CSE, respectively. SARS is essential protein in cytoplasm,

Table 3. Identified proteins that were found to appear and disappear in a narrow pH range 4-7 (L, linear).

Spot No.	Gene name	Protein name	pI	MW (kDa)	Accession number[a]	Sequence coverage[b] (%)	Protein level ratio (fold change)[c]		
							Control/ Control	CSE 3%/ Control	CSE 5%/ Control
C1	MYOC	Trabecular meshwork-induced glucocorticoid response protein	5.5	54.886	12585283	93.14	–	1	3.12
C2	MMP13	Matrix metalloproteinase 13	5.4	53.921	27805999	87.81	–	1	4.51
C3	CHGA	Chromogranin-A	4.7	50.031	30794306	78.68	–	1	3.13
C4	KRT8	Keratin, type II cytoskeletal 8	5.1	42.396	125109	91.02	–	1	1.51
C5	ANXA4	Annexin A4	5.5	35.889	48374083	81.38	–	1	4.85
C6	FN	Fibronectin	6.4	35.486	15866750	86.47	–	1	2.83
C7	POU5F1	POU domain, class 5, transcription factor 1	5.7	38.290	27807049	76.31	–	1	1.91
C8	LUM	Lumican precursor	5.9	38.757	27806853	75.41	–	1	2.30
C9	SPARC	Secreted protein acidic and rich in cysteine	4.7	34.717	27806147	78.12	–	1	3.18
C10	RPSA	40S ribosomal protein SA	4.8	32.897	27805981	81.29	–	1	3.66
C11	CALB1	Calbindin	4.6	29.835	115392	83.64	–	1	1.84
D1	LOC480645	Similar to epsilon isoform of 14-3-3 protein	4.6	29.174	57091321	91.37	–	–	1
D2	AHSP	Alpha-hemoglobin-stabilizing protein	4.8	10.718	Q865F8	75.39	–	–	1
D3		Myoglobin precursor	6.90	17.078	217580	77.81	–	–	1
D4	PLA2G2D2	Putative calcium-dependent phospholipase A2	6.0	15.241	54606395	91.24	–	–	1
D5	DQB4	Major histocompatibility complex class II	5.7	9.793	1754825	82.36	–	–	1
D6	DBI	Acyl-CoA-binding protein	6.1	10.045	P07107	64.35	–	–	1
E1	PYCARD	Apoptosis-associated speck-like protein containing a CARD	5.3	21.918	27807409	69.59	1	0.35	–
E2		Similar to ferritin H subunit	5.3	11.671	28189182	91.38	1	0.61	–
F1	CL43	Collectin-43 precursor	5.0	33.616	50355694	86.12	1	–	–
F2	ACTA2	Actin, aortic smooth muscle	5.2	42.009	296472858	89.34	1	–	–
F3	MYOC	Myocilin	5.4	34.059	4760473	78.51	1	–	–
F4		Actin-binding protein capG	6.17	38.876	29468984	76.35	1	–	–
F5		Beta A3 crystallin	6.0	25.128	50262256	81.68	1	–	–
F6	AKAP5	A-kinase anchor protein 5	5.1	47.879	27806325	81.02	1	–	–

[a]Accession code refers to the SWISS-2DPAGE database; [b]Mass tolerance in protein identification through PMF experiment was 10 ppm; [c]Protein expression level in each growth phases compared with N4 phase. Expression level in N4 phase was set at 1.
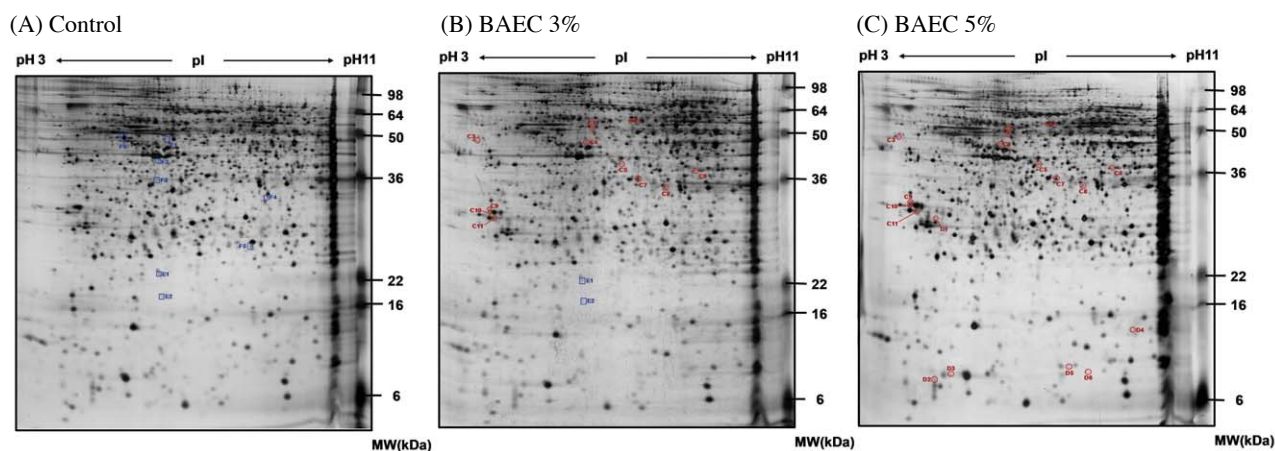
(A) Control   (B) BAEC 3%   (C) BAEC 5%

Figure 2. Silver stained 2-D SDS-PAGE gels showing 25 protein spots listed in Table 2. Proteins marked with the red circle were found to be appearing by CSE treatment [○]; and the blue indicated proteins that were disappeared [□]. Control, (A); CSE 3% treatment (B); CSE 5% treatment (C).

which is responsible for the aminoacylation of cognate transfer-RNAs with serine specifically. In an earlier study, SARS mediated transcriptional repression has been reported during vascular development. That is, SARS protein located in nucleus repressed VEGF-A mRNA transcription, thereby permitting normal vascular development. Moreover, the correlation between VEGF and apoptosis in cigarette smokers has been demonstrated recently[33]. They proposed that a certain factor derived from cigarette smoking may induce VEGF mutations and apoptosis. Based on this earlier report and our data, we hypothesize that it might be due to the reason that SARS down-regulation by CSE exposure results in induction of VEGF and its mutation and it eventually activates apoptosis pathway in BAECs. However, it still remains an unresolved questions that whether SARS directly interacts with VEGF gene promoter and modulates its transcription level, or acts by an indirect mediator. In addition, it is also to be checked whether SARS repression activates VEGF mutation directly or not.

Regulation of signal transduction pathway

S-arrestin is one of the cytosolic proteins that can only form complexes with transmembrane receptors after agonist stimulation and phosphorylation by the G protein coupled receptor kinase[34,35]. That is, it can be understandable that arrestin binding to the receptor blocks further G protein-mediated signaling. It is currently believed that most endogenous transmembrane receptors appear to signal in a balanced fashion using arrestin and G protein-mediated pathway. We postulate that arrestin reduction and/or interaction interference between arrestin and its receptors could stimu-

late G protein-mediated pathway. Eventually, signaling results in the activation of apoptosis responses. We observed significant repression of S-arrestin (SAG, D13) when cells were exposed to CSE 5%, but not at 3%. Arrestin repression seems likely to be associated with CSE-dose. To date, there have been very few reports which regard arrestin as carcingogens[36,37]. They have demonstrated that over-regulating arrestin expression induced the growth and apoptosis. The behavior of arrestin of 5% CSE treated BAECs in the present study show good agreement with that of earlier studies.

Internal ROS production and cell death

NADH dehydrogenase (Ubiquinone) iron-sulfur protein 3 (NDUFS3, B14) displayed a reduction in abundance of about 10-20% for CSE treated cells. NDUF3 is core subunit of the mitochondrial membrane respiratory chain NADH dehydrogenase (complex I) that is believed to belong to the minimal assembly required for catalysis. It has been reported that disorders associated with complex I deficiency mostly lead to multisystem disorders thereby affecting brain, muscle and the heart[38]. Especially, in terms of ATP production chain, complex I deficiency may lead to an increase in the reactive oxygen species (ROS) production in mitochondrial. Excessive ROS formation may induce the over expression of a variety of genes and transcription of death effector genes, as has already been studied well[39]. Therefore, we can conclude that reduced NDUFS3 levels following CSE exposure may indicate induced cell death signaling, apoptosis.

In the cell mediated immune system, apoptotic cells and their components can be urgently digested, which
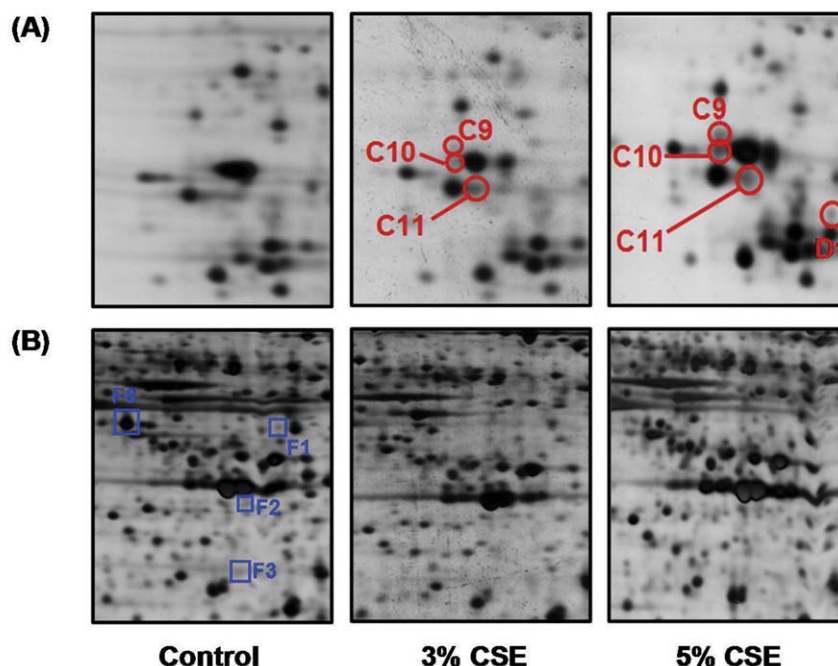
Figure 3. Close-up images of representative 2-DE gel images showing intensity changes; (A) Appearance and (B) Disappearance.

is essential for avoiding an innate immune responses, such as inflammatory responses[25,40]. Therefore, apoptotic cell expresses their patterned probe on the cell surface during apoptotic cellular processes that allow the selective endocytosis of an abnormal cell. One of distinguishable feature of apoptosis is that the endomembrane structure is degraded[41], suggesting that critical changes in secretory pathway might occur, for example, dispersal of Golgi complex and inhibition of trafficking during apoptosis. It has been observed that apoptotic cell failed to accumulate target protein in Golgi apparatus under destroying early secretory pathway (ER-Golgi trafficking)[42]. In line with their observation, our proteome analysis also explains the reduced abundance of Transmembrane emp24 domain-containing protein 9 (TMED9, B16). TMED9 is involved in vesicular protein trafficking, mainly in the early secretory pathway. Therefore, the reduced TMED9 may contribute to impair membrane trafficking by CSE expose in BAECs, thereby leading to apoptosis.

Reduction of tumor-inducer proteins

Our results have also shown a significant reduction in Annexin A2 (BCL2L14, B20), and Dihydrofolate recuctase (DHFR, B21) when cells were exposed to higher dose of (5%) of CSE. First of all, the effects of cigarette smoking on lung cancer has been previously

reported that Annexin A2 and Dihydroforate reductase were highly expressed in a majority of tumors[43,44]. Annexin A2 has been implicated in cell-cell adhesion and in plasminogen activation and may function as a cell surface receptor in a predominantly membrane pattern. Tetrahydrofolate and its derivatives play an important role in cell proliferation and growth. As a key factor, DHFR has an essential role in the regulation of tetrahydrofolate function. That is, since DHFR is responsible for the levels of tetrahydrofolate, the inhibition of DHFR can limit proliferation of cell that is characteristic of cancer. Hence, reduced Annexin A2 and DHFR levels following high-dose CSE expose may indicate induced cell death signaling.

Comparison of protein profiles with narrow range pH: Linear pH 4-7

Spots of interest with reproducible intensity and pattern differences observed in the broad range pH 3-11 2-DE gels were mainly monitored and identified in the acidic regions. Therefore, CSE induced protein difference was analyzed using linear pH 4-7 strips and a detail spot analysis was performed. Table 2 listed proteins, which showed up-and down-regulated expression under exposure to CSE. Among them, overexpressed spots identified Interferon-alpha/beta receptor chain (IFNAR, a6)[27], Vascuolar ATP synthase sub-

unit H (ATP6V1H, a10), Cartilage oligomeric matrix protein (COMP, a11)[33], Glial fibrillary acidic protein (GFAP, a17)[45] and Adenosine deaminase (ADA, a19)[29,46] were observed in both pH conditions. Major classification of the identified proteins was involved in immune response, transcription/translation and cytoskeletal-related proteins. Furthermore, we were particularly interested in those proteins that were found to appear and disappear on 2-DE gels after CSE treatment. Overall, twenty-five proteins were found in the pH 4-7 analytical range, out of which 17 spots appeared and 16 spots disappeared after CSE treatment (Figure 2 and Table 3). Functional classification of the identified proteins revealed cytoskeletal-related proteins (MYOC, MMP13, KRT8, FN, ACTA2, Myoglobin precursor, Actin binding protein capG), secretory proteins (CHGA, SPARC), metabolic processes (CALB1, PLA2G2D2, DBI), transcription/translation related proteins (POU5F1, RPSA, AKAP5) and proteins involved in immune system (DQB4, CL43). Many of the identified proteins were involved in extracullular structure of cells, which were found to appear under 3% and 5% CSE treatment. Our results indicate that structural protein in apoptotic signaling response could serve as an inducer. In particular, Matrix metalloproteinase 13 (MMP13, C2) was found to be appearing at CSE 3% and spot intensity showed more than 4-fold abundance compared to base level upon cellular exposure to 5% CSE. This protein is mainly expressed in the skeleton as required for restructuring the collagen matrix. As understanding of MMP13 activity, it has been suggested that MMP-dependent extracellular proteolysis seems likely to be important to several neuronal cellular activities[45]. While, Mycilin (MYCO, F3), which is believed to have a role in cytoskeletal function disappeared when cells were exposed to CSE at both 3% and 5% (Figure 3). Interestingly, it was previously shown that MYOC aggregates could induce ER stress and lead to apoptosis[47]. Moreover, cigarette smoking affects to induce an unfolded protein response in the human lung[48]. Therefore, the observed disappearance of MYOC might be a result of protein aggregation/misfolding by CSE expose.

In conclusion, various protein profiles of BEACs were identified after exposure to cigarette smoke extract at different concentrations (0, 3% and 5%) and investigated by 2-DE-based proteome analysis. In broad pH range 2-DE gel analysis, most of the proteins identified are involved in apoptosis, inflammation, transcription, signal transduction, ROS production, cell death progress, tumorization and extracullular structure of cell. Major protein change shown in up-regulation was DNA methyltransferase, while NADH dehydrogenase iron-sulfur protein 3 (NDUFS3) was significantly down-regulated at 5% CSE treatment. Areas of interest with reproducible spots observed in pH 3-11 2-DE gels were mainly monitored in the acidic regions. Analysis of pH 4-7 provided details of spot analysis in that area. From the comparative proteome analysis in narrow pH range 4-7, several proteins were evaluated. More specifically, we focused on the identification of disappearance and appearance of spots, as well as up- and down-regulation of spot intensities under different concentration (0, 3 and 5%) of CSE. These findings can be potentially used as early biomarkers to indicate risks of cigarette smoke related diseases and also offer prospects for the development of new therapeutic and diagnostic approaches.

Materials & Methods

Preparation of cigarette smoke extract

The aqueous cigarette smoke extract (CSE) was prepared as described in an earlier publication[49], by using a Erlenmeyer flask containing 30 mL of phosphate-buffered saline (PBS, pH 7.4). The cigarette smoke was bubbled through this solution with the help of a tube. A commercially available cigarette (THIS Plus, Korean Tobacco and Ginseng Company, Inc., Daejeon, Korea) was installed at one end of the tube and the smoke from a lit cigarette was allowed to bubble slowly through the PBS by continuous aspiration with a water vacuum pump connected to the side-arm of the flask. After consecutive pumping with 3 lit cigarettes, the resulting suspension was filtered through a 0.2 μm filter, and then stored in aliquots at $-70°C$ for different experiments. In the absence of any standard for CSE three cigarettes smoked into 30 mL medium were taken to yield 100% cigarette smoke extract (CSE) and this was applied to endothelial cultures after dilution with culture medium. The CSE concentrations used in the present study are 0, 3 and 5%.

Cell culture and CSE treatment

Bovine aortic endothelial cells (BAECs) were isolated as described previously[50] and were maintained in MEM supplemented with 5% NCS at 37°C under 5% CO_2-20% O_2 air. The endothelial cells were evaluated by light microscopy and by a positive indirect immunofluorescence test for the von Willebrand factor VIII complex. Cells between 5th and 7th passages were used in the present study. BAECs were further incubated for 24 hours in MEM supplemented with 0.5% NCS. For CSE treatment, BAECs cultured at 80% confluency were then subjected to CSE at 0, 3 and 5% concentrations for different times.

Sample preparations for two-dimensional electrophoresis

The cells as described in above were detached from the culture dishes, transferred to a 15 mL centrifuge tube and were pelleted by centrifugation at 500 g for 5 min at room temperature. The pellet was resuspended in 1.5 mL ice-cold PBS, transferred to an Eppendorf tube, and again centrifuged for 10 s at 15,000 g. The pellet was then resuspended in $1 \times$ packed cell volume of cold 25 mM Tris-HCl, pH 7.4, containing 0.5 mM EDTA, 0.5 mM EGTA, and 1 mM PMSF by flicking the tube and leaving it on ice for 15 min. The supernatant was discarded and the pellet was resuspended in 2/3 pcv of ice-cold 20 mM Hepes, pH 7.5, containing 20 mM KCl, 1.5 mM $MgCl_2$, 25% glycerol, 420 mM NaCl, 1 mM EDTA, 1 mM EGTA, 1 mM DTT, 0.25 M sucrose, and 1 mM PMSF. After incubation on ice for 30 min while stirring, the suspension was centrifuged at 15,000 g for 5 min at 4°C. The protein concentration was determined by Bio-Rad protein assay kit (Hercules, CA, USA) using bovine serum albumin as a standard. The supernatants were kept at −80°C until used for 2-DE. 700 μg proteins were resuspended in rehydration solution (8 M urea, 2% w/v CHAPS, 0.005% w/v bromophenol blue; final volume, 350 μL). Urea and 3-[(3-cholamidopropyl) dimethyl-ammonio]-1-propanesulfonate (CHAPS), Tris, dithiothreitol (DTT), bromophenol blue, Triton X-100 and sodium dodecyl sulfate (SDS) were purchased from Sigma Chemical Co. (St. Louis, MO, USA).

2-DE and image analysis

In the first step of 2-DE, IEF was performed on a Pharmacia Biotech IPGphor Electrophoresis System at 20 °C. Non-linear pH 3-11 and linear pH 4-7 immobilized gel strips (18 cm, Amersham Pharmacia Biotech, Uppsala, Sweden) were rehydrated overnight by placing the strips gel-side-down in sample-containing rehydration solution in the IPGphor strip holder and covering with the DryStrip Cover Fluid (Amersham Pharmacia Biotech, NJ, USA). The samples were loaded with intracellular protein concentrations of 700 μg for 2-DE analytic gels with Seablue plus2 marker (Invitrogen, CA, USA). IEF was performed for 2 h at 500 V, for 0.5 h at 1000 V, for 0.5 h at 2000 V, for 0.5 h at 4000 V, and finally maintained 70000 V*h at 8000 V in the IPGphor for analytical and preparative gels. Next, the IPG gel strips were equilibrated for 15 min in equilibration solution (50 mM Tris-HCl, pH 8.8, urea 6 M, glycerol 30% v/v, SDS 2% w/v, bromophenol blue trace), in 1% w/v DTT for 15 min, and then in 2.5% w/v iodoacetamide for 15 min. Equilibrated gel strips were placed on a 12.5% polyacrylamide gel, and the second dimensional separation was carried out using a PRO TEAN II Xi cell system (Bio-rad, Ca, USA) in a cold chamber at 4°C. SDS-PAGE was carried out at 30 mA/gel for 12 h until the bromophenol blue reached at the bottom of the gel. Silver stained gels were scanned using UMAX powerlook 1100 scanner. ImageMaster software v 4.01 (Amersham Pharmacia Biotech, NJ, USA) was used for the gel image analysis including quantification of the spot intensities which is done on a volume basis (values were calculated form the integration of spot optical intensity over the spot area).

MALDI-TOF mass spectrometric analysis and protein identification

MALDI-TOF mass spectrometry analysis was carried out as previous protocol with some modifications[51]. Enzymatic digestions were performed overnight at 37 °C in stationary incubator using 10-15 μg/mL of sequencing grade modified trypsin (Proma, WI, USA) in 25 mM ammonium bicarbonate (pH 8.0). In the gel, digested peptide fragments were extracted from gel pieces using solution prepared by adding 5% v/v trifluoroacetic acid to 50% v/v acetonitrile followed by vortexing for 1 h. After repeating it three times, solute materials including peptide fragments were dried down by vacuum centrifugation. Ziptip column (Millipore, Bedford, USA) in which C_{18} resin is fixed at the end of the tip was used to eliminate impurities of samples. The peptide solution was prepared with an equal volume of saturated α-cynao-4-hydroxy-cinnamic acid solution in 50% ACN/0.1% TFA on a sample plate of MALDI-TOF mass spectrometer. Protein analyses were performed using MALDI-TOF mass spectrometry system (Voyager DE-STR, PE Biosystem, Framingham, MA). Spectra were calibrated using a matrix and tryptic autodigestion ion peaks as internal standards. Peptide mass fingerprints were analyzed using the MS-Fit (http://prospector.ucsf.edu/). The identification of a protein with respective theoretical parameters (pI, molecular mass) was accepted if the peptide mass matched with a mass tolerance within 10 ppm. The accessibility of such data has been revolutionized by the use of internet protocols such as SWISS-2D-PAGE (http://www.expasy.org/).

Conflict of Interest   The authors declare no conflict of interest.

References

 1. Morrow, J. D. *et al*. Increase in circulating products of lipid peroxidation (F2-isoprostanes) in smokers. Smoking as a cause of oxidative damage. *N Engl J Med* **332**: 1198-1203 (1995).
 2. Bermudez, E. A., Rifai, N., Buring, J. E., Manson, J. E. & Ridker, P. M. Relation between markers of systemic vascular inflammation and smoking in women. *Am J Cardiol* **89**:1117-1119 (2002).
 3. Leanderson, P. & Tagesson, C. Cigarette smoke-induced DNA damage in cultured human lung cells: role of hydroxyl radicals and endonuclease activation. *Chem Biol Interact* **81**:197-208 (1992).
 4. Renne, R. A. *et al*. Effects of flavoring and casing ingredients on the toxicity of mainstream cigarette smoke in rats. *Inhal Toxicol* **18**:685-706 (2006).
 5. Chen, Z. & Boreham, J. Smoking and cardiovascular disease. *Semin Vasc Med* **2**:243-252 (2002).
 6. Sundar, I. K., Nevid, M. Z., Friedman, A. E. & Rahman, I. Cigarette smoke induces distinct histone modifications in lung cells: implications for the pathogenesis of COPD and lung cancer. *J Proteome Res* **13**:982-996 (2014).
 7. Di Cello, F. *et al*. Cigarette smoke induces epithelial to mesenchymal transition and increases the metastatic ability of breast cancer cells. *Mol Cancer* **12**:90 (2013).
 8. Pierson, T., Learmonth-Pierson, S., Pinto, D. & van Hoek, M. L. Cigarette smoke extract induces differential expression levels of beta-defensin peptides in human alveolar epithelial cells. *Tob Induc Dis* **11**:10 (2013).
 9. Xi, S. *et al*. Cigarette smoke mediates epigenetic repression of miR-487b during pulmonary carcinogenesis. *J Clin Invest* **123**:1241-1261 (2013).
10. Micale, R. T. *et al*. Oxidative stress in the lung of mice exposed to cigarette smoke either early in life or in adulthood. *Arch Toxicol* **87**:915-918 (2013).
11. Du, B., Altorki, N. K., Kopelovich, L., Subbaramaiah, K. & Dannenberg, A. J. Tobacco smoke stimulates the transcription of amphiregulin in human oral epithelial cells: evidence of a cyclic AMP-responsive element binding protein-dependent mechanism. *Cancer Res* **65**:5982-5988 (2005).
12. Ma, D., Chow, S., Obrocka, M., Connors, T. & Fischer, I. Induction of microtubule-associated protein 1B expression in Schwann cells during nerve regeneration. *Brain Res* **823**:141-153 (1999).
13. Wang, Y. *et al*. Human bronchial epithelial and endothelial cells express alpha7 nicotinic acetylcholine receptors. *Mol Pharmacol* **60**:1201-1209 (2001).
14. Chang, C. C. *et al*. Proteomic analysis of proteins from bronchoalveolar lavage fluid reveals the action mechanism of ultrafine carbon black-induced lung injury in mice. *Proteomics* **7**:4388-4397 (2007).
15. Fach, E. M. *et al*. *In vitro* biomarker discovery for atherosclerosis by proteomics. *Mol Cell Proteomics* **3**:1200-1210 (2004).
16. Plymoth, A. *et al*. Rapid proteome analysis of bronchoalveolar lavage samples of lifelong smokers and never-smokers by micro-scale liquid chromatography and mass spectrometry. *Clin Chem* **52**:671-679 (2006).
17. Battershill, J. M. The Multiple Chemicals and Actions Model of carcinogenesis. A possible new approach to developing prevention strategies for environmental carcinogenesis. *Hum Exp Toxicol* **24**:547-558 (2005).
18. George, J. & Shukla, Y. Pesticides and cancer: insights into toxicoproteomic-based findings. *J Proteomics* **74**: 2713-2722 (2011).
19. Stinn, W. *et al*. Lung inflammatory effects, tumorigenesis, and emphysema development in a long-term inhalation study with cigarette mainstream smoke in mice. *Toxicol Sci* **131**:596-611 (2013).
20. Vallotton, M. B., Dolci, W., Gerber-Wicht, C. & Fischer, J. A. Action of calcitonin gene-related peptide on rat aortic smooth muscle. *Eur J Pharmacol* **166**: 219-222 (1989).
21. Carnevali, S. *et al*. Cigarette smoke extract induces oxidative stress and apoptosis in human lung fibroblasts. *Am J Physiol Lung Cell Mol Physiol* **284**: L955-963 (2003).
22. Gorg, A., Obermaier, C., Boguth, G. & Weiss, W. Recent developments in two-dimensional gel electrophoresis with immobilized pH gradients: wide pH gradients up to pH 12, longer separation distances and simplified procedures. *Electrophoresis* **20**:712-717 (1999).
23. Hall, A. The cytoskeleton and cancer. *Cancer Metastasis Rev* **28**:5-14 (2009).
24. Fritz, G., Just, I. & Kaina, B. Rho GTPases are overexpressed in human tumors. *Int J Cancer* **81**:682-687 (1999).
25. Hengartner, M. O. The biochemistry of apoptosis. *Nature* **407**:770-776 (2000).
26. Bursch, W., Kleine, L. & Tenniswood, M. The biochemistry of cell death by apoptosis. *Biochem Cell Biol* **68**:1071-1074 (1990).
27. Wang, L. *et al*. Induction of secondary apoptosis, inflammation, and lung fibrosis after intratracheal instillation of apoptotic cells in rats. *Am J Physiol Lung Cell Mol Physiol* **290**:L695-L702 (2006).

28. Gakis, C. Adenosine deaminase (ADA) isoenzymes ADA1 and ADA2: diagnostic and biological role. *Eur Respir J* **9**:632-633 (1996).

29. Theatre, E. *et al*. Overexpression of CD39 in mouse airways promotes bacteria-induced inflammation. *J Immunol* **189**:1966-1974 (2012).

30. Hodge, D. R. *et al*. Interleukin-6 regulation of the human DNA methyltransferase (HDNMT) gene in human erythroleukemia cells. *J Biol Chem* **276**:39508-39511 (2001).

31. Fujiwara, K., Okamura-Ikeda, K. & Motokawa, Y. Mechanism of the glycine cleavage reaction. Further characterization of the intermediate attached to H-protein and of the reaction catalyzed by T-protein. *J Biol Chem* **259**:10664-10668 (1984).

32. Zhong, Z. *et al*. L-Glycine: a novel antiinflammatory, immunomodulatory, and cytoprotective agent. *Curr Opin Clin Nutr Metab Care* **6**:229-240 (2003).

33. Rahmani, A., Alzohairy, M., Khadri, H., Mandal, A. K. & Rizvi, M. A. Expressional evaluation of vascular endothelial growth factor (VEGF) protein in urinary bladder carcinoma patients exposed to cigarette smoke. *Int J Clin Exp Pathol* **5**:195-202 (2012).

34. Yamaki, K. *et al*. Structural organization of the human S-antigen gene. cDNA, amino acid, intron, exon, promoter, in vitro transcription, retina, and pineal gland. *J Biol Chem* **265**:20757-20762 (1990).

35. Gurevich, V. V. *et al*. Arrestin interactions with G protein-coupled receptors. Direct binding studies of wild type and mutant arrestins with rhodopsin, beta 2-adrenergic, and m2 muscarinic cholinergic receptors. *J Biol Chem* **270**:720-731 (1995).

36. Zou, L., Yang, R., Chai, J. & Pei, G. Rapid xenograft tumor progression in beta-arrestin1 transgenic mice due to enhanced tumor angiogenesis. *FASEB J* **22**:355-364 (2008).

37. Wang, P. *et al*. Beta-arrestin 2 functions as a G-protein-coupled receptor-activated regulator of oncoprotein Mdm2. *J Biol Chem* **278**:6363-6370 (2003).

38. Saada, A. *et al*. Mutations in NDUFAF3 (C3ORF60), encoding an NDUFAF4 (C6ORF66)-interacting complex I assembly protein, cause fatal neonatal mitochondrial disease. *Am J Hum Genet* **84**:718-727 (2009).

39. Tominaga, H., Kodama, S., Matsuda, N., Suzuki, K. & Watanabe, M. Involvement of reactive oxygen species (ROS) in the induction of genetic instability by radiation. *J Radiat Res* **45**:181-188 (2004).

40. Savill, J. Apoptosis. Phagocytic docking without shocking. *Nature* **392**:442-443 (1998).

41. Kerr, J. F., Wyllie, A. H. & Currie, A. R. Apoptosis: a basic biological phenomenon with wide-ranging implications in tissue kinetics. *Br J Cancer* **26**:239-257 (1972).

42. Namekawa, M. *et al*. Mutations in the SPG3A gene encoding the GTPase atlastin interfere with vesicle trafficking in the ER/Golgi interface and Golgi morphogenesis. *Mol Cell Neurosci* **35**:1-13 (2007).

43. Lokman, N. A., Ween, M. P., Oehler, M. K. & Ricciardelli, C. The role of annexin A2 in tumorigenesis and cancer progression. *Cancer Microenviron* **4**:199-208 (2011).

44. Chen, C. Y. *et al*. Thymidylate synthase and dihydrofolate reductase expression in non-small cell lung carcinoma: the association with treatment efficacy of pemetrexed. *Lung Cancer* **74**:132-138 (2011).

45. Mannello, F., Luchetti, F., Falcieri, E. & Papa, S. Multiple roles of matrix metalloproteinases during apoptosis. *Apoptosis* **10**:19-24 (2005).

46. Gakis, C. The low cost of the adenosine deaminase assay. *Chest* **110**:1376-1377 (1996).

47. Yam, G. H., Gaplovska-Kysela, K., Zuber, C. & Roth, J. Aggregated myocilin induces russell bodies and causes apoptosis: implications for the pathogenesis of myocilin-caused primary open-angle glaucoma. *Am J Pathol* **170**:100-109 (2007).

48. Kelsen, S. G. *et al*. Cigarette smoke induces an unfolded protein response in the human lung: a proteomic approach. *Am J Respir Cell Mol Biol* **38**:541-550 (2008).

49. Su, Y., Han, W., Giraldo, C., De Li, Y. & Block, E. R. Effect of cigarette smoke extract on nitric oxide synthase in pulmonary artery endothelial cells. *Am J Respir Cell Mol Biol* **19**:819-825 (1998).

50. Kim, H. P. *et al*. Nongenomic stimulation of nitric oxide release by estrogen is mediated by estrogen receptor alpha localized in caveolae. *Biochem Biophys Res Commun* **263**:257-262 (1999).

51. Gorg, A. IPG-Dalt of very alkaline proteins. *Methods Mol Biol* **112**:197-209 (1999).